JNMS Journal of Nippon Medical School https://www.nms.ac.jp/sh/jnms/

Original

Midazolam and Dexmedetomidine Promoted Migration of Human Lung Adenocarcinoma A549 Cells

Anna Ishikawa, Masae Iwasaki, Masahiro Tomihari, Makiko Yamamoto and Masashi Ishikawa

Department of Anesthesiology and Pain Medicine, Graduate School of Medicine, Nippon Medical School, Tokyo, Japan

Background: The numerous studies of the effects of intravenous anesthetics on cancer have suggested potential effects on cell migration and postoperative outcomes. This study compared the direct effects of midazolam and dexmedetomidine on A549 human lung adenocarcinoma cells.

Methods: A549 cells were exposed for 2 hr to midazolam (5, 10, 15, 20 μM), dexmedetomidine (1, 10, 100 nM), or medium alone as a naïve control. Cell viability changes were assessed with a wound healing assay, adenosine triphosphate (ATP) analysis, and cell counting kit-8 (CCK) assay. Tumor metastasis–related gene expression was assessed by a polymerase chain reaction (PCR) array and qRT-PCR. Hypoxia-inducible factor (HIF-1α), angiotensin-converting enzyme 2 (ACE2), matrix metalloproteinase (MMP9), and β-catenin expressions were assessed by immunofluorescence staining.

Results: Midazolam treatments promoted cell migration and metabolism but suppressed cell proliferation, whereas D treatments promoted cell migration only and had no effect on metabolism or cell proliferation. The PCR array of cancer-related genes revealed that five genes were upregulated by midazolam treatment relative to naïve controls: Frizzled-1 (FZD1), AKT serine/threonine kinase 2 (AKT2), E2F transcription factor 1 (E2F1), Fos proto-oncogene, AP-1 transcription factor subunit (FOS), and tumor protein p53 (TP53). Two genes were upregulated in the dexmedetomidine group: the CRK proto-oncogene, adaptor protein (CRK) and FZD1.

Conclusions: These findings clarify how dexmedetomidine and midazolam treatments affect lung cancer prognoses. Our data suggest that midazolam rather than dexmedetomidine should be recommended for lung cancer surgery.

(J Nippon Med Sch 2026; 93 (2): 161–172. https://doi.org/10.1272/jnms.JNMS.2026_93-210)

Keywords: cancer biology, intravenous anesthetics, dexmedetomidine, midazolam, ACE2

Introduction

Malignant cancer is the most common cause of death in Japan, accounting for 400,000 deaths annually[1]. Among cancer deaths, lung cancer, especially non-small cell lung cancer, is the most common cause[1]. In Japan, surgical resection under general anesthesia is the first-line therapy for early-stage lung cancer[2]. Although the potential effects of perioperative anesthetics on cancer outcomes have been studied, the effects remain unclear[3,4].

A retrospective analysis of anesthesia types used during surgery for breast and colon cancers indicated that intravenous anesthesia resulted in a better survival rate than inhalational anesthesia[5]. The anesthetics midazolam and dexmedetomidine are widely used as intravenous drugs in general anesthesia, and several research groups have investigated the anticancer effects of these drugs. In an in vitro experiment, midazolam inhibited proliferation of hypopharyngeal squamous cell carcinoma cell by sup-

Correspondence to Masae Iwasaki, masae-a@nms.ac.jp
https://doi.org/10.1272/jnms.JNMS.2026_93-210
Received: August 9, 2025; Accepted: December 17, 2025
Copyright © 2026 The Medical Association of Nippon Medical School. This is an open access article under the CC BY-NC-ND 4.0 license (https://creativecommons.org/licenses/by-nc-nd/4.0/).

pressing transient receptor potential melastatin 7 (TRPM 7)[6]. Another group reported that midazolam suppressed proliferation and migration of hepatocellular carcinoma cells by upregulating miR-124-3p and downregulating PIM-1, Pim-1 proto-oncogene, and serine/threonine kinase[7]. Wang et al.[11] reported that dexmedetomidine administration promoted proliferation and migration of human lung carcinoma cells and neuroglioma cells by upregulating B-cell leukemia/lymphoma 2 (Bcl-2) and B-cell lymphoma-extra large (Bcl-xL).

Several cancer-related biomarkers correlate with cancer prognosis, including hypoxia-inducible factor 1α (HIF-1 α), matrix metalloproteinase 9 (MMP9), and β-catenin as pro-cancer factors, and angiotensin-converting enzyme 2 (ACE2) as an anticancer factor[8]. A study using human lung adenocarcinoma A549 cells found that midazolam 5–20 μM inhibited the mitogen-activated protein kinase (MAPK) pathway and MMP expression[9]. Treatment with dexmedetomidine stimulated expressions of HIF-1α and MMP9 in A549 cells[10].

These studies of the effects of intravenous anesthetics on A549 cells did not comprehensively investigate key cancer-related biomarkers, such as HIF-1α, ACE2, MMP9, and β-catenin, or include a comparative analysis of their effects. The present study thus compared the effects of two common intravenous anesthetics, midazolam and dexmedetomidine, on human lung adenocarcinoma A549 cells.

Materials and Methods

Cell Culture

Cells of the human-authenticated lung adenocarcinoma cell line A549 (RCB0098, RIKEN BioResource Research Center, Kyoto, Japan) were cultured in RPMI 1640 medium (Thermo Fisher Scientific [TFS], Tokyo) containing 10% fetal bovine serum and 1% penicillin/streptomycin (TFS) and maintained in a humidified incubator at 37°C with a 5% CO_2 atmosphere.

Midazolam and Dexmedetomidine Treatments

Midazolam and dexmedetomidine were obtained from Sandoz Group (Tokyo). In accordance with a previous study, the concentrations administered to cell cultures were 5, 10, 15, and 20 μM for midazolam and 1, 10, and 100 nM for dexmedetomidine, yielding seven treatment groups, designated M5, M10, M15, M20, D1, D10, and D 100[11]. A naïve control (NC) group of cells receiving no anesthetics was also established. Cells were exposed to each treatment for 2 hr, which is a reasonable approximation of the duration of lung cancer surgery.

Cell Counting Kit-8 Cell Proliferation Test

Cells were plated at an approximate density of 5×10^3 per well on 96-well plates and allowed to adhere for 24 hr. The cells were then exposed to each midazolam or dexmedetomidine concentration or control treatment for 2 hr and allowed to sit for another 24 hr. The cell counting kit-8 (CCK) proliferation test was then performed, following the manufacturer's manual (Dojindo Laboratories, Kumamoto, Japan), by using a SpectraMax i3x microplate reader (Molecular Devices, Tokyo).

Cell Migration Test (Wound-Healing Assay)

Cells were plated at 3×10^5 cells per well of a three-well insert (Culture-Insert 3 well; ibidi, Fitchburg, WI, USA) on 35-mm cell culture petri dishes and rested for 24 hr. The cells were then exposed to the predetermined midazolam or dexmedetomidine concentration for 2 hr. After another 24 hr, the insert was removed, and the gap closure was examined by optical microscopy (CKX31; Olympus, Tokyo) at 20× magnification (LCAch N; Olympus). To calculate the gap closure rate, the images were assessed with the Image J 1.54i image analysis tool (U.S. National Institutes of Health, Bethesda, MD, USA).

Cell Metabolism Test (ATP Analysis)

Cells were plated at an approximate density of 5×10^3 cells per well on 96-well plates and allowed to adhere for 24 hr. Next, the cells were exposed to each midazolam or dexmedetomidine concentration for 2 hr and allowed to sit for another 24 hr. An adenosine triphosphate (ATP) analysis was performed using a CellTiter-Glo 2.0 Cell Viability Assay (Promega Japan, Tokyo), following the manufacturer's instructions, and the SpectraMax i3x microplate reader.

RNA Extraction

Total RNA was extracted from 80% confluent cells on 60-mm cell culture petri dishes at 6 hr after the 2-hr anesthesia or control exposure, using an RNeasy Mini Kit and QIAshredder column (Qiagen) according to the manufacturer's instructions. The RNA quantity and quality were assessed using a NanoDrop microvolume spectrophotometer (TFS). Samples with an A260/A280 ratio >1.8 were considered to be of sufficient quality for further analysis. For these analyses, 1 mg of each total RNA sample was converted into cDNA with the use of a high-capacity cDNA reverse transcription kit (TFS).

Polymerase Chain Reaction Array

Polymerase chain reaction (PCR) array analysis was performed, and the results were analyzed using the 'TaqMan Array Human Molecular Mechanisms of Cancer 96-well plate' and the QuantStudio 5 system (TFS), following the manufacturer's protocol. The array plate layout is shown in **Supplementary Table 1**. Out of three endogenous control candidates, the glyceraldehyde-3-phosphate dehydrogenase (GAPDH) mRNA with the most stable Ct value was selected as the endogenous control to evaluate each relative expression ratio, using the comparative 2−ΔΔCt method. PCR array analysis was performed using ExpressionSuite ver. 1.3 software (TFS), and a cluster analysis was conducted to determine the average linkage between clusters based on the Euclidian distance.

Validation qRT-PCR

Some representative genes (HIF-1α, MMP9, β-catenin, cadherin-1, and ACE2) were subjected to a further quantitative reverse transcription (qRT)-PCR using TaqMan primers and TaqMan Fast Advanced Mastermix (TFS) with QuantStudio 5 software. GUSB was selected as endogenous control. The TaqMan primer (TFS) numbers were Hs00153153_m1 for HIF-1α, Hs00957562_m1 for MMP9, Hs00355045_m1 for β-catenin, Hs01023895_m1 for CDH1, Hs01085333_m1 for ACE2, and Hs00939627_m 1 for GUSB. PCR analysis was performed using the ExpressionSuite ver. 1.3 software.

Immunofluorescence Study

At 24 hr after seeding 3×10^5 cells on a 13-mm cover glass in each well of a 24-well plate, the cells were exposed to midazolam or dexmedetomidine at the above-described concentrations for 2 hr and then allowed to rest for 24 hr. Next, the cells were fixed with 4% paraformaldehyde and blocked with 10% normal donkey serum (Merck Chemicals, Amsterdam, The Netherlands) and then incubated overnight at 4°C with each of the following primary antibodies: rabbit anti-ACE2 (1:200; Abcam, Tokyo), rabbit anti-HIF-1α (1:200; Novus Biologicals, Centennial, CO), rabbit anti-MMP9 (1:200; Cell Signaling Technology [CST], Tokyo) and rabbit anti-β-catenin (1: 200; CST). The samples were incubated with a conjugated secondary antibody (Alexa Fluor 568; TFS) and co-stained with Vectashield mounting medium containing DAPI (TFS). Six areas of each slide were randomly selected for imaging under a microscope (BX53; Olympus) at 40× magnification (DP74; Olympus), followed by an analysis using the Image J 1.54i tool.

Western Blotting

To investigate HIF-1α expression with dexmedetomidine or midazolam, western blotting was performed with our established protocol (Iwasaki, 2016 #32). At 24 hr after seeding 0.8×10^6 cells on a 60-mm cell culture petri-dishes, the cells were exposed to midazolam or dexmedetomidine at the above-described concentrations for 2 hr and then allowed to rest for 24 hr. Cell protein samples were extracted using 1 mM dithiothreitol cell lysis buffer (CST). Protein samples were assessed with Nanodrop, and 40 μg of each sample was electrophoresed on a 10% Mini-PROTEAN TGX Precast Gel (Bio-Rad Laboratories, Inc., Tokyo, Japan). After electrophoresis, the samples were transferred to a polyvinylidene difluoride (PVDF) membrane by using the transblot turbo system (Bio-Rad Laboratories). Membranes were blocked with blocking buffer (Bio-Rad Laboratories) for 1 hr at room temperature and then incubated overnight at 4°C with rabbit anti-HIF-1α (1:200; Novus Biologicals, Centennial, CO) followed by horseradish peroxidase (HRP)−linked anti-rabbit secondary antibody (CST; 1:1,000) for 1 hr. The loading control was the constitutively expressed protein GAPDH (CST, anti-rabbit monoclonal, 1:5,000). The blots were washed with TBST for 5 min three times followed by one wash with TBS and were visualized using the Laemmli sample buffer (Bio-Rad Laboratories). Densitometry analysis was carried out using ImageQuant LAS 4000 mini (Cytiva, Tokyo, Japan). The results are presented as the ratio of the protein of interest to a control housekeeping protein for analysis with the Image J 1.54i tool.

Statistical Analysis

All numerical data are presented as scatterplots or mean ± SD. We determined that a group size of six samples was needed to show a 30% change with 80% power at 5% significance. Statistical analyses were performed using one-way analysis of variance (ANOVA), followed by a post hoc Tukey−Kramer test, using Prism 9.0 software (GraphPad Software, San Diego, CA, USA). For the analysis of the PCR array results, the false discovery rate was set as 0.1 using the program QVALUE 2.0 (http://github.com/jdstorey/qvalue, accessed May 7, 2025). In all experiments, a P value of <0.05 was considered to indicate statistical significance.

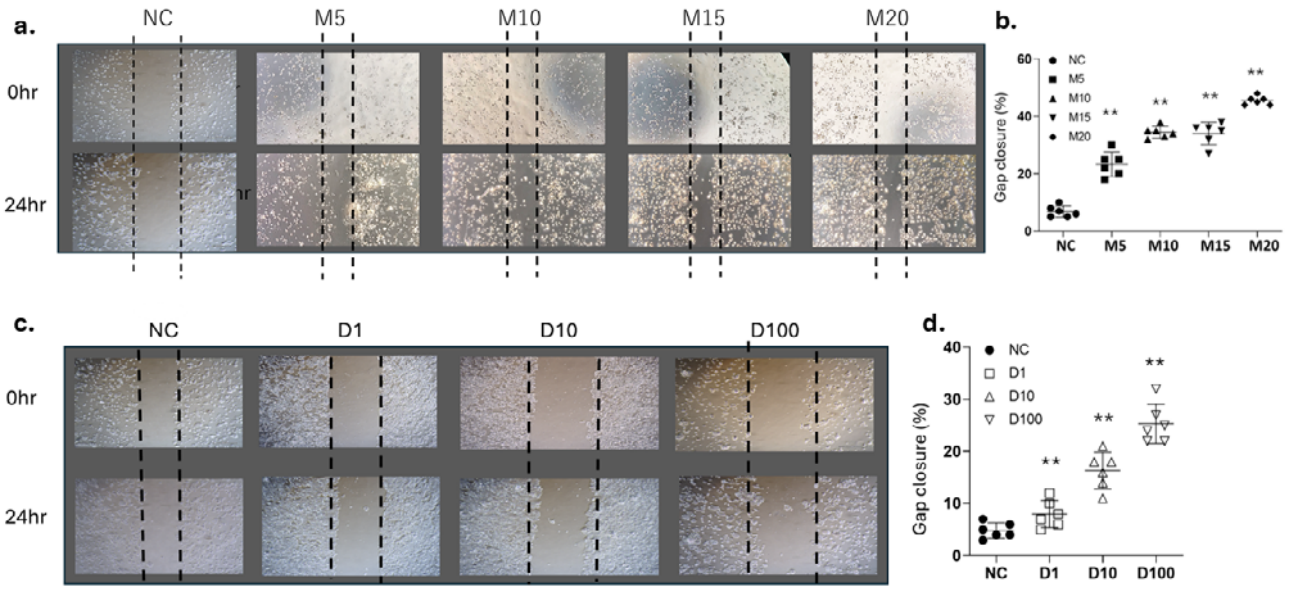

Figure 1 Wound healing assay analysis after 2-hr exposure to midazolam (M) or dexmedetomidine (D)
(a) Representative M treatment images. (b) Statistical analysis of the wound healing assay with M treatment. (c) Representative D treatment images. (d) Statistical analysis of the wound healing assay with D treatment.
Dots: naïve controls (NCs); black squares: treatment with 5 μM of M (M5); black triangles: M10; black downward triangles: M15; black diamonds: M20; white squares: treatment with 1 μM of D (D1 treatment); white triangles: D10; white downward triangles: D100.
**p<0.01, n=6 samples, mean ± SD, one-way ANOVA followed by post hoc Tukey test vs. NC group.

Results

Cell Viability Tests

Wound healing assay: Midazolam and dexmedetomidine promoted A549 cell migration

The final score of the wound healing assay (WHA) was calculated as the sum of independently measured migration and proliferation values. The results are shown in **Figure 1**. Each of the four M treatments (M5, M10, M15, and M20) significantly enhanced migration of A549 human lung adenocarcinoma cells, as compared with the NC treatment (NC 6.83 ± 1.77 vs. M5 23.3 ± 3.9, M10 34.5 ± 1.89, M15 34.0 ± 3.6, and M20 45.5 ± 1.38, all p<0.0001; **Figure 1a and 1b**). Similarly, all three D treatments (D1, D10, and D100) significantly increased cell migration as compared with the NC treatment (NC 4.83 ± 1.34 vs. D1 8.00 ± 2.38 vs. D10 16.3 ± 3.19 vs. D100 26.3 ± 3.44, all p <0.0001; **Figure 1c and 1d**).

CCK assay: Lower midazolam concentrations inhibited A549 cell proliferation

The CCK assay was performed to assess cell proliferation changes (**Figure 2**). As compared with the NC treatment, the M5 and M10 treatments significantly suppressed cell proliferation, whereas the M15 and M20 treatments yielded no significant changes (NC 1.04 ± 0.05 vs. M5 0.83 ± 0.12, p=0.0018; NC 1.04 ± 0.05 vs. M10 0.79 ± 0.08, p=0.0003; **Figure 2a**). There were no significant differences in CCK assay results between the dexmedetomidine treatment groups and NC treatment group (mean ± SD, n = 6 samples; NC 1.00 ± 0.05 vs D1 1.00 ± 0.08, p>0.05; vs D10 1.19 ± 0.12, p>0.05; D100 1.07 ± 0.12, p>0.05; D1 vs D10, p=0.0130; D1 vs D100, p=0.0584; **Figure 2b**).

The combined results of the WHA and CCK assay indicate that the M treatments promoted migration but suppressed cell proliferation, whereas D treatments promoted migration but had no effect on cell proliferation.

ATP analysis: Midazolam treatment suppressed ATP metabolism in A549 cells

Figure 3 shows the results of ATP analysis as a measure of ATP metabolism in the cells. All M treatments significantly reduced cell metabolism, as compared with the NC treatment (NC 1.00 ± 0.26 vs. M5 0.47 ± 0.23, M10 0.51 ± 0.13, M15 0.51 ± 0.17, and M20 0.39 ± 0.11, p= 0.0021, 0.0044, 0.0048, 0.0004, respectively; **Figure 3a**). No D treatment induced a significant change, as compared with NC treatment in cell ATP metabolism (**Figure 3b**).

These data on cell viability suggest that midazolam treatment induced metabolic stress and growth inhibition, affecting the overall function of cells, whereas dexmedetomidine treatment selectively acted on cell mi-

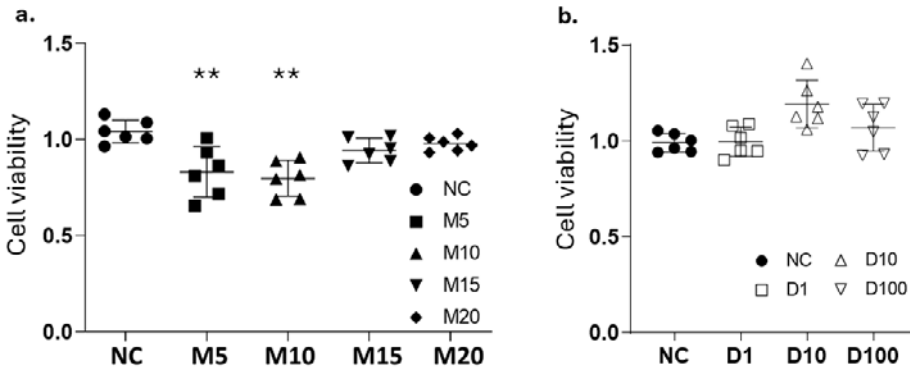

Figure 2 Cell count assay analysis after 2-hr anesthesia exposure
(a) M, (b) D. **p<0.01, n=6 samples, mean±SD, one-way ANOVA followed by post hoc Tukey test vs. NC group.
Dots: naïve control; black squares: treatment with 5 μM of M (M5); black triangles: M10; black downward triangles: M15; black diamonds: M20; white squares: treatment with 1 μM of D (D1); white triangles: D10; white downward triangles: D100.
NC: naïve control treatment.

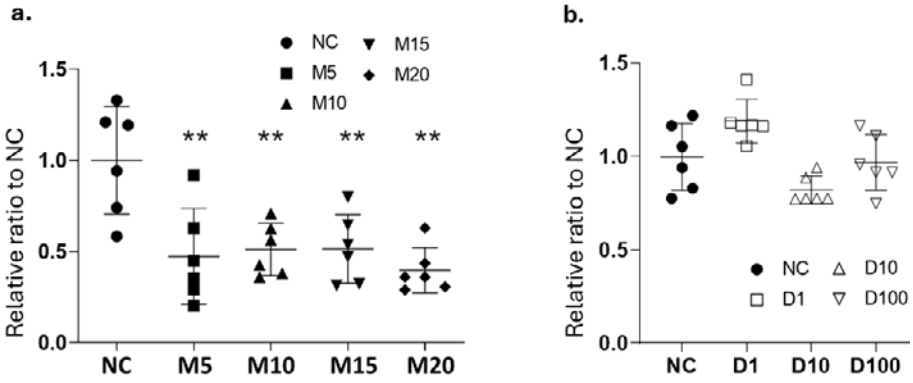

Figure 3 ATP analysis after 2-hr anesthesia exposure
(a) M, (b) D. **p<0.01, n=6 samples, mean ±SD, one-way ANOVA followed by post hoc Tukey test vs. NC group.
Dots: Naïve control treatment (NC); black squares: treatment with 5 μM of M (M5); black triangles: M10; black downward triangles: M15; black diamonds: M20; white squares: treatment with 1 μM of D (D1); white triangles: D10; white downward triangles: D100.

gration signals without affecting metabolism or growth.

PCR array: Midazolam and dexmedetomidine changed cancer-related mRNAs in A549 cells

A PCR array was used to examine cancer-related genes after M10 or D100 treatment, and the results are shown in **Table 1**. Cells in the M10 treatment group exhibited significant upregulation of five genes, as compared with those of the NC group: frizzled class receptor 1 (FZD1) (NC 1.00 ± 0.33 vs. M10 1.94 ± 0.35, p=0.002), AKT serine/threonine kinase 2 (AKT2) (NC 1.00 ± 0.26 vs. M10 1.61 ± 0.21, p=0.001), E2F transcription factor 1 (E2F1) (NC 1.00 ± 0.26 vs. M10 1.85 ± 0.39, p=0.002), Fos proto-oncogene, AP-1 transcription factor subunit (FOS) (NC 1.00 ± 0.32 vs. M10 2.01 ± 0.32, p=0.002), and tumor protein p53 (TP53) (NC 1.00 ± 0.29 vs. M10 1.00 ± 0.27, p=0.001).

Cells in the D100 treatment group showed significant upregulation of two genes: FZD1 (NC vs. D100 2.11 ± 0.43, p<0.0001) and CT10 regulator of kinase (CRK) (NC 1.00 ± 0.39 vs. D100 3.03 ± 0.69, p=0.001). FZD1 was thus the only gene significantly upregulated by both the M10 and D100 treatments.

The PCR array data showed that midazolam treatment increased the expression of several genes—AKT2, E2F1, FOS, TP53, and FZD1—which support activation of survival and proliferation signals. In contrast, dexmedetomidine treatment elevated expressions of CRK and

Table 1 Expression Profiling of Cancer-Related Genes in Response to Midazolam and Dexmedetomidine Treatment

a: Genes upregulated only with midazolam treatment

	Relative changes			p-value (q-value)		
Gene	NC	M10	D100	NC vs. M10	NC vs. D100	M10 vs. D100
AKT2	1.000 ± 0.267	1.619 ± 0.210	1.237 ± 0.205	0.001 (0.039)	0.205 (0.645)	0.029 (0.250)
E2F1	1.000 ± 0.269	1.855 ± 0.396	1.683 ± 0.377	0.002 (0.044)	0.010 (0.124)	0.669 (0.999)
FOS	1.000 ± 0.327	2.010 ± 0.325	0.910 ± 0.519	0.002 (0.044)	0.920 (0.999)	0.001 (0.039)
TP53	1.000 ± 0.299	1.711 ± 0.272	1.008 ± 0.184	0.001 (0.039)	0.998 (0.999)	0.001 (0.039)

b: Genes upregulated only with dexmedetomidine treatment

	Relative changes			p-value (q-value)		
Gene	NC	M10	D100	NC vs. M10	NC vs. D100	M10 vs. D100
CRK	1.000 ± 0.395	2.173 ± 1.173	3.030 ± 0.693	0.053 (0.403)	0.001 (0.044)	0.181 (0.645)

c: Genes upregulated by both midazolam and dexmedetomidine treatment

	Relative changes			p-value (q-value)		
Gene	NC	M10	D100	NC vs. M10	NC vs. D100	M10 vs. D100
FZD1	1.000 ± 0.337	1.944 ± 0.353	2.113 ± 0.432	0.002 (0.044)	0.000 (0.039)	0.724 (0.999)

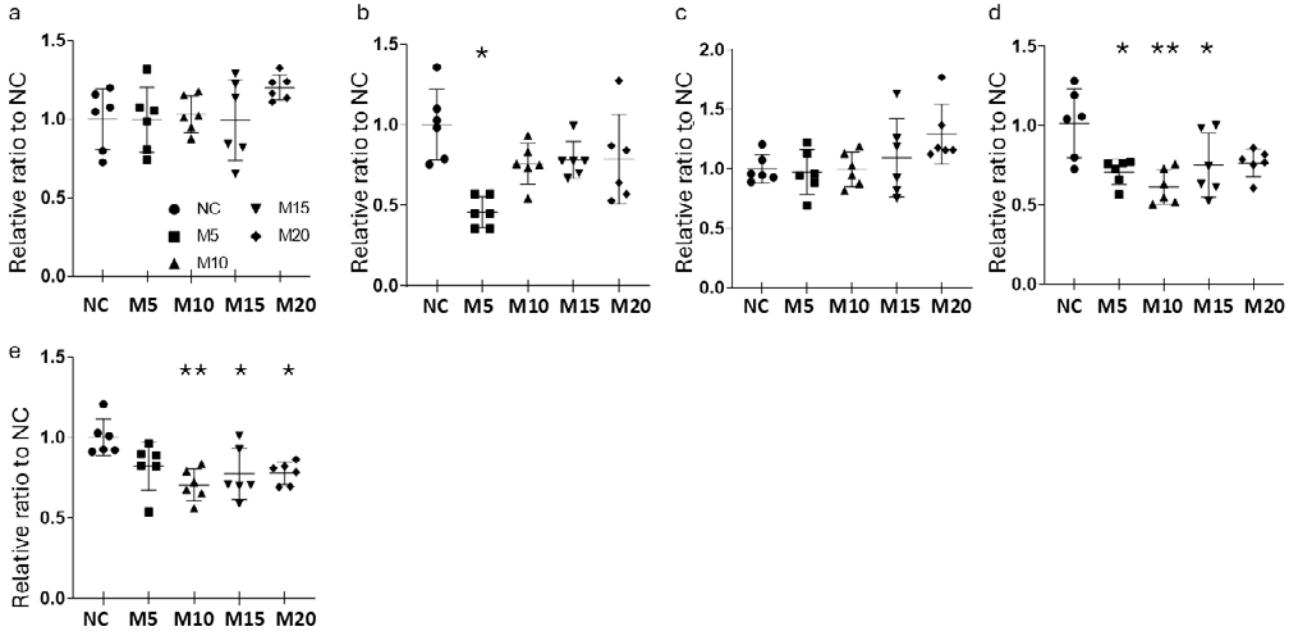

Figure 4 RT-PCR analysis after 2-hr midazolam exposure

(a) HIF-1α. (b) MMP9. (c) β-catenin. (d) ACE2. (e) cadherin-1. **p<0.01, *p<0.05. n=6 samples, mean ± SD, one-way ANOVA followed by post hoc Tukey test vs. the naïve control (NC) group.

Dots: naïve control treatment (NC); black squares: treatment with 5 μM of M (M5); black triangles: M10; black downward triangles: M15; black diamonds: M20.

ACE2: angiotensin-converting enzyme 2; HIF-1α: hypoxia-inducible factor 1α; MMP9: matrix metalloproteinase 9.

FZD1, indicating activation of pathways related to cell motility and migration.

RT-PCR: Midazolam decreased expressions of pro-cancer markers and anticancer markers

qRT-PCR was performed to confirm gene expression changes of several biomarkers after the M treatments (**Figure 4**) and D treatments (**Figure 5**), as compared with

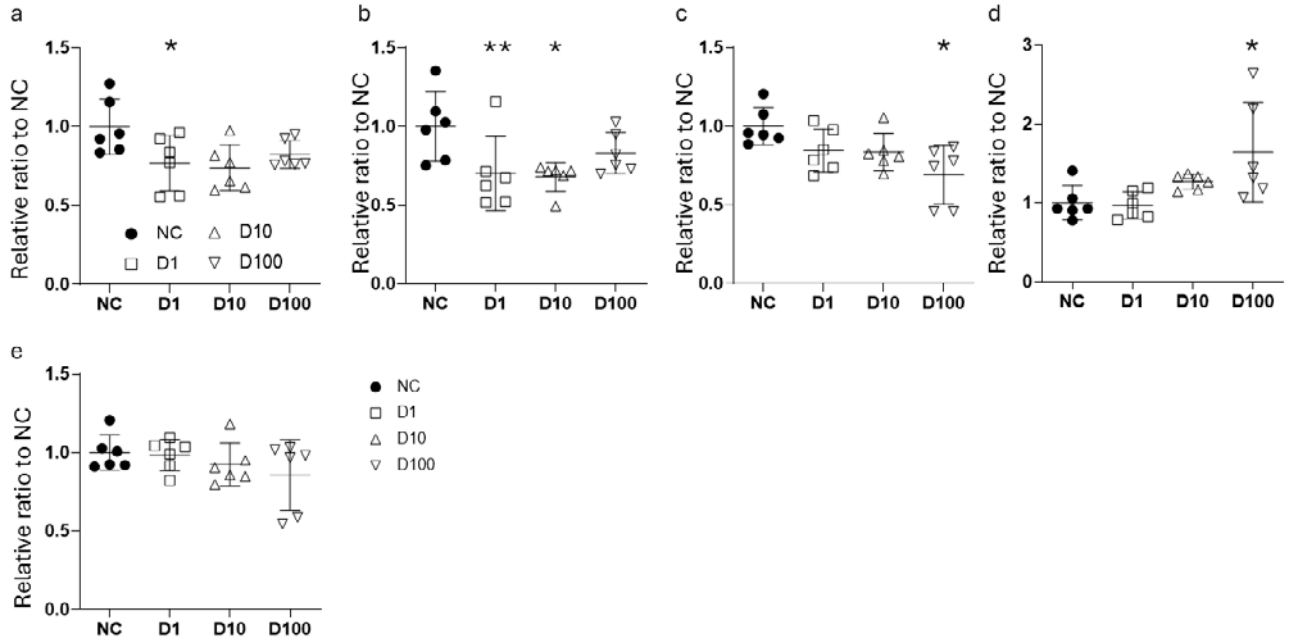

Figure 5 RT-PCR analysis after 2-hr dexmedetomidine exposure
(a) HIF-1α. (b) MMP9. (c) β-catenin. (d) ACE2. (e) cadherin-1. **p<0.01, *p<0.05. n=6 samples, mean ± SD, one-way ANOVA followed by post hoc Tukey test vs. naïve control (NC) group.
Dots: naïve control treatment (NC); white squares: treatment with 1 μM of D (D1); white triangles: D10; white downward triangles: D100.
ACE2: angiotensin-converting enzyme 2; HIF-1α: hypoxia-inducible factor 1α; MMP9: matrix metalloproteinase 9.

Table 2 RT-PCR results of representative genes

a: qRT-PCR analysis after 2 hr dexmedetomidine administration

	Relative changes				P value		
Gene	NC	D1	D10	D100	NC vs. D1	NC vs. D10	NC vs. D100
ACE2	1.000 ± 0.522	0.910 ± 0.074	1.216 ± 0.226	1.584 ± 0.698	0.816	0.121	0.002
HIF-1α	1.000 ± 0.176	0.769 ± 0.177	0.739 ± 0.145	0.825 ± 0.088	0.986	0.898	0.987
CDH1	1.000 ± 0.112	0.984 ± 0.099	0.924 ± 0.137	0.857 ± 0.226	0.998	0.821	0.383
β-catenin	1.000 ± 0.119	0.846 ± 0.138	0.836 ± 0.119	0.691 ± 0.185	0.271	0.224	0.006
MMP-9	1.000 ± 0.122	0.622 ± 0.210	0.581 ± 0.079	1.205 ± 0.190	0.010	0.004	0.246

b: qRT-PCR analysis after 2 hr midazolam administration

	Relative changes					P value			
Gene	NC	M5	M10	M15	M20	NC vs. M5	NC vs. M10	NC vs. M15	NC vs. M20
ACE2	1.000 ± 0.522	0.539 ± 0.097	0.447 ± 0.080	0.546 ± 0.146	0.557 ± 0.063	0.083	0.004	0.102	0.137
HIF-1α	1.000 ± 0.176	0.769 ± 0.177	0.739 ± 0.145	0.825 ± 0.088	0.825 ± 0.088	>0.9999	0.998	>0.9999	0.341
CDH1	1.000 ± 0.112	0.821 ± 0.149	0.705 ± 0.099	0.774 ± 0.160	0.777 ± 0.070	0.118	0.003	0.029	0.032
β-catenin	1.000 ± 0.119	0.972 ± 0.187	0.996 ± 0.145	1.095 ± 0.330	1.293 ± 0.250	0.999	>0.9999	0.942	0.177
MMP-9	1.000 ± 0.122	0.458 ± 0.096	0.756 ± 0.128	0.750 ± 0.068	0.786 ± 0.227	0.000	0.168	0.253	0.274

the NC treatment (**Table 2**). M treatments did not significantly change the expression of HIF-1α, a pro-cancer biomarker, as compared with the NC treatment (NC 1.00 ± 0.28 vs. M5 0.95 ± 0.25, p>0.05; NC vs. M10 0.94 ± 0.10, vs. M15 1.00 ± 0.20, and vs. M20 1.03 ± 0.07, all p>0.05; **Figure 4a**). Expression of the cancer metastasis biomarker MMP9 was significantly decreased in the M5 group but not in the other M treatment groups (NC 1.00±0.20 vs. M 5 0.55 ± 0.10, p=0.0048; M5 0.55 ± 0.10 vs. M15 0.91 ± 0.12, p=0.0269; **Figure 4b**).

β-catenin expression did not significantly change in any M treatment group (NC 1.00 ± 0.30, M5 1.11 ± 0.21,

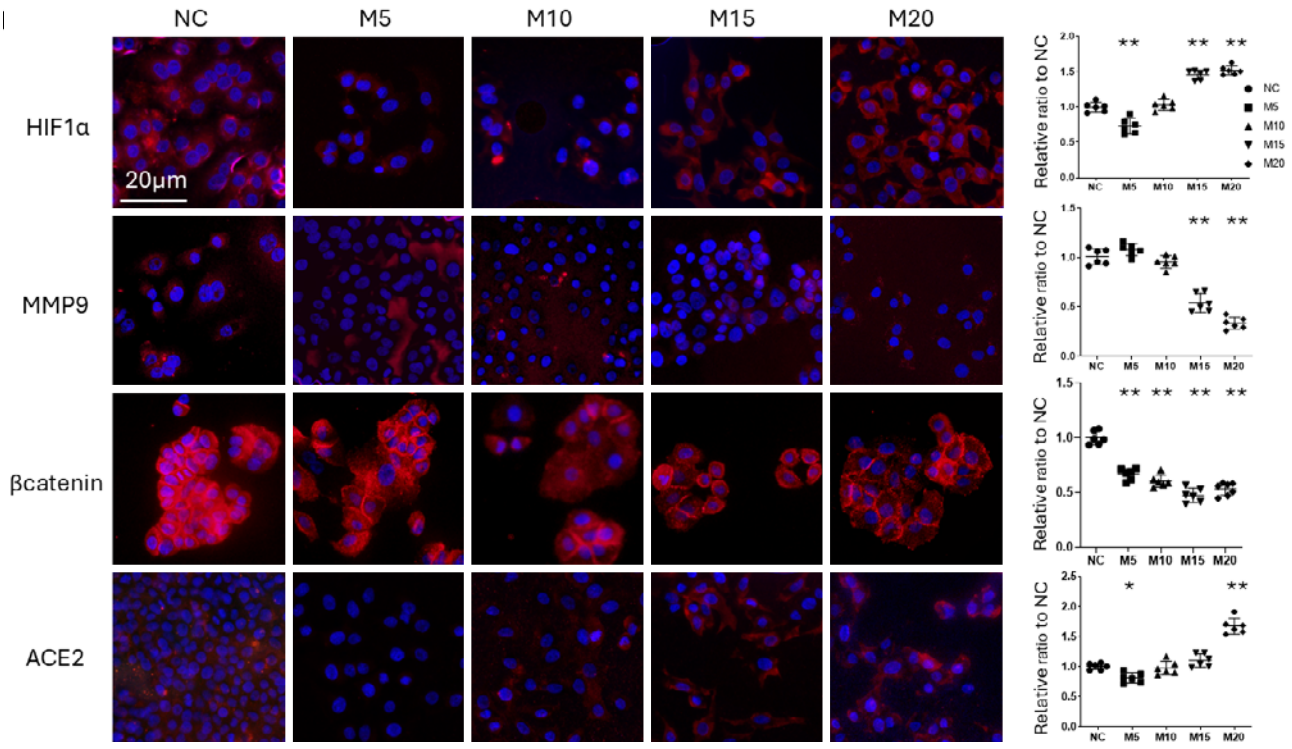

Figure 6 Representative images of immunofluorescence staining of A549 cells treated with control (left) and M treatments, counterstained with DAPI (blue); ×40 magnification, scale bar = 20 μm
Data are plots and mean ± SD. *p<0.05, **p<0.01, n=6 samples, one-way ANOVA followed by post hoc Tukey test vs. the naïve control (NC) group.
Dots: naïve controls; black squares: treatment with 5 μM of M (M5); black triangles: M10; black downward triangles: M15; black diamonds: M20.

M10 1.09 ± 0.04, M15 1.18 ± 0.14, M20 1.34 ± 0.15, all p> 0.05; **Figure 4c**). The anticancer biomarker ACE2 was downregulated in all M treatment groups (NC 1.00 ± 0.23 vs. M5 0.70 ± 0.10, p=0.0249; vs. M10 0.57 ± 0.11, p= 0.0006; vs. M15 0.68 ± 0.08, p=0.0142; and vs. M20 0.67 ± 0.01, p=0.0106; **Figure 4d**). Cadherin 1 (a cell adhesion factor) was downregulated at higher midazolam concentrations (**Figure 4e**). Midazolam treatment had limited effects on the mRNA transcription levels of anti- and pro-cancer factors.

RT-PCR: Dexmedetomidine treatment suppressed expressions of pro-cancer markers and upregulated expression of an anti-cancer biomarker

As compared with the NC group, the D treatments resulted in reduced expressions of HIF-1α (NC 1.00 ± 0.28 vs. D1 0.90 ± 0.10, p>0.05; vs. D10 0.83 ± 0.06, p>0.05; vs. D100 0.56 ± 0.11, p=0.0026; **Figure 5a** and **Table 2b**). Expressions of MMP9 and β-catenin were significantly downregulated in the D100 group (MMP9: NC 1.00 ± 0.20 vs. D10 0.67 ± 0.08, p=0.0283 [**Figure 5b**]; β-catenin: NC 1.00 ± 0.30 vs. D100 0.45 ± 0.12, p=0.0007 [**Figure 5 c**]). ACE2 expression was significantly upregulated in the D100 group (NC 1.00 ± 0.23 vs. D100 1.54 ± 0.10, p= 0.0176; **Figure 5d**). Cadherin 1 expression did not change with dexmedetomidine administration (**Figure 5e**). These findings suggest that dexmedetomidine treatment suppressed pro-cancer factor genes at the mRNA transcription level.

Immunofluorescent staining: Midazolam treatment suppressed expressions of MMP9 and β-catenin in A549 cells

Figure 6 shows representative images of the immunofluorescent staining results. HIF-1α expression was significantly upregulated in the M15 and M20 groups (HIF-1α: NC 1.00 ± 0.06 vs. M5 0.73 ± 0.09, vs. M10 1.03 ± 0.07, vs. M15 1.45 ± 0.06; and vs. M20 1.51 ± 0.06, p< 0.0001, 0.9603, <0.0001, <0.0001, respectively). MMP9 and β-catenin expressions were both significantly decreased in all M treatment groups (MMP9: NC 1.01 ± 0.06 vs. M5 1.07 ± 0.05, vs. M10 0.95 ± 0.05, vs. M15 0.54 ± 0.08, and vs. M20 0.33 ± 0.05, p=0.4752, 0.7171, <0.0001, <0.0001, respectively; β-catenin: NC 1.00 ± 0.05 vs. M5 0.66 ± 0.04, vs. M10 0.60 ± 0.05, vs. M15 0.47 ± 0.05, and vs. M20 0.53 ± 0.05, all p<0.0001).

ACE2 expression was significantly upregulated in the

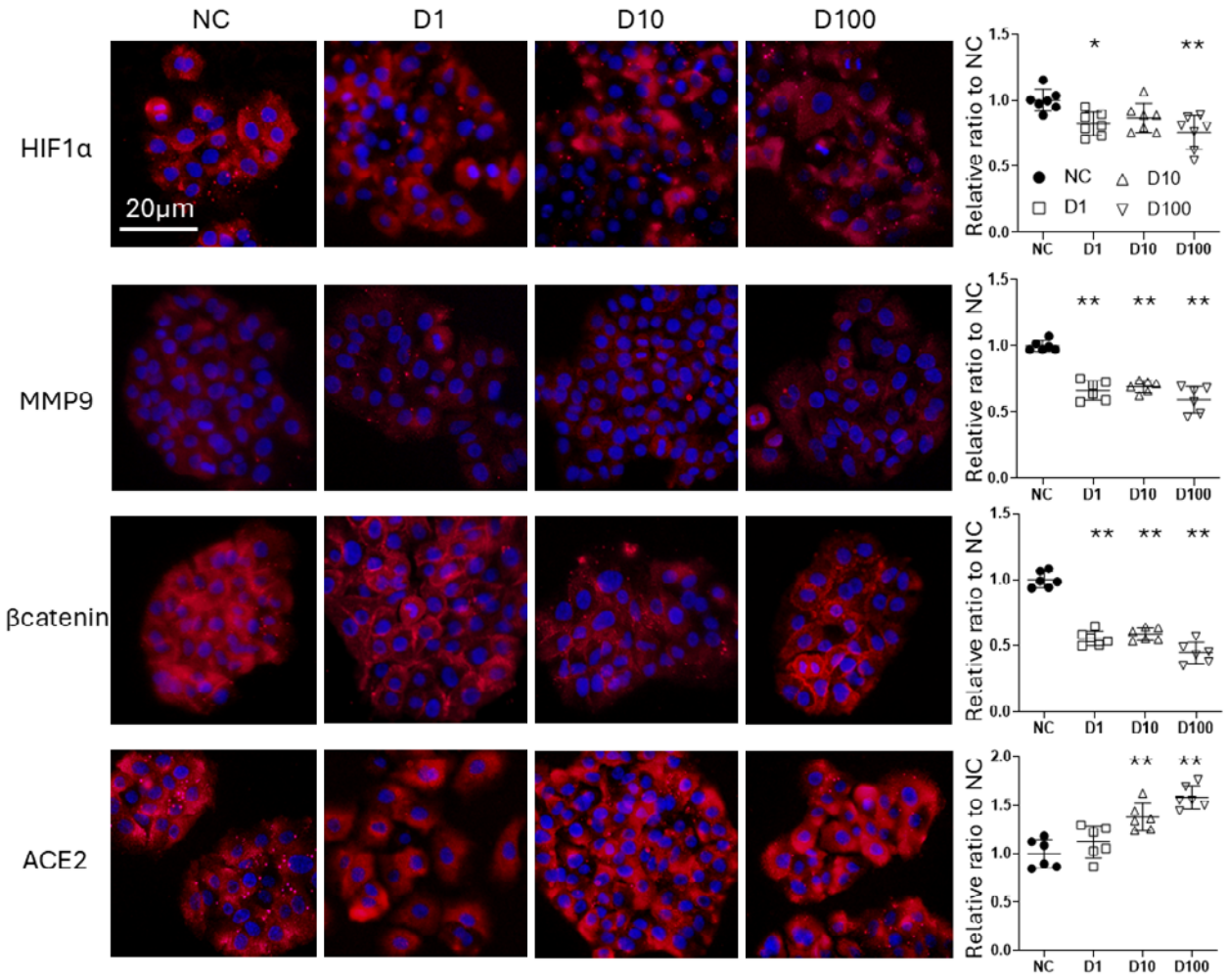

Figure 7 Representative images of immunofluorescence staining of A549 cells treated with control (left) and M treatments, counterstained with DAPI (blue); ×40 magnification, scale bar = 20 μm
Data are plots and mean ± SD. *p<0.05, **p<0.01, n=6 samples, one-way ANOVA followed by post hoc Tukey test vs. the naïve control (NC) group.
Dots: naïve controls; white squares: treatment with 1 μM of D (D1); white triangles: D10; white downward triangles: D100.

higher M treatment groups (NC 1.00 ± 0.06 vs. M5 0.73 ± 0.09, vs. M10 1.03 ± 0.07, vs. M15 1.45 ± 0.06, and vs. M 20 1.51 ± 0.06, p=0.0280, 0.9898, 0.4602, <0.0001, respectively). Midazolam treatment partially reduced expression of proteins related to migration and invasion, while HIF-1α resulted in a biphasic change.

Immunofluorescent staining: Dexmedetomidine treatment suppressed expressions of pro-cancer biomarkers in A549 cells

Representative images for the D treatment groups are shown in **Figure 7**. The D1 and D100 groups showed significantly decreased expressions of HIF-1α (NC 1.00 ± 0.07 vs. D1 0.82 ± 0.08, p=0.0185; vs. D100 0.75 ± 0.11, p= 0.0011). Similarly, MMP9 and β-catenin expressions were significantly suppressed in all three D treatment groups (MMP9: NC 1.00 ± 0.03 vs. D1 0.66 ± 0.06, vs. D10 0.69 ± 0.04, and vs. D100 0.59 ± 0.09, all p<0.0001; β-catenin: NC 1.00 ± 0.05 vs. D1 0.55 ± 0.05, vs. D10 0.57± 0.04, and vs. D100 0.44± 0.07, all p<0.0001).

In contrast, ACE2 expression was significantly enhanced in all D treatment groups (NC 1.00 ± 0.13 vs. D1 1.12 ± 0.15, vs. D10 1.37 ± 0.12, and vs. D100 1.58 ± 0.10, 0.4853, 0.0011, <0.0001, respectively). Dexmedetomidine treatment appeared to inhibit invasion-related molecules at the protein level as well.

Western blotting: Dexmedetomidine treatment suppressed HIF-1α expression

Western blotting of HIF-1α was used to confirm overall protein expression in cells. Dexmedetomidine treatment suppressed HIF-1α expression, which was consistent with the IF results (data not shown; representative image in **Supplementary Figure 1**).

Discussion

Our findings indicate that midazolam administration suppressed proliferation and ATP synthesis of A549 cells, whereas both midazolam and dexmedetomidine treatment promoted cell migration. The PCR array of cancer-related genes demonstrated that midazolam upregulated expressions of five genes (AKT2, E2F1, FOS, TP53 and FZD1) and that dexmedetomidine upregulated expressions of four genes (AKT2, FOS, TP53 and FZD1). We set the duration of all midazolam and dexmedetomidine treatments at 2 hr, which is the typical duration of surgery for lung cancer.

Our results revealed that treatment with midazolam (0–20 μM) promoted migration and inhibited proliferation of A549 cells. Clinical doses of midazolam range from 15 to 50 μM, so the concentrations used in this study were lower than those used clinically. One in vitro study showed that midazolam at higher concentrations and a longer exposure time (25–400 μM for 48 hr) suppressed migration and proliferation of A549 cells[11], whereas lower midazolam concentrations (0.01–10 μM) produced no changes. Another study reported that midazolam (5, 10, 20 μM) inhibited cell proliferation by blocking cell transformation via TGFβ[12]. The present findings suggest that promotion of migratory ability by midazolam was neither ATP-dependent nor MMP-dependent but rather signal pathway–dependent.

We observed that midazolam treatment promoted migration but suppressed proliferation of lung adenocarcinoma cells. Among the pro-cancer biomarkers, HIF-1α is known to be activated in hypoxia, to promote cancer cell proliferation and migration, and to positively correlate with tumor progression in many types of cancer[13]. MMP9 can stimulate cancer invasion, metastasis, and angiogenesis[14,15]. MMP9 overexpression in clinical pathological samples is related to cancer metastasis and is a cancer-prognosis factor[16,17]. Midazolam (5–20 μM) was reported to suppress MMP9 expression by inhibiting the p38 MAPK pathway[9]. β-catenin is the key factor of the Wnt/β-catenin pathway, which controls cancer proliferation[18], cancer formation[19], and cancer cell survival[20]. ACE2 is a clinically favorable prognostic biomarker[21] that can inhibit angiogenesis[22] by controlling HIF-1α, MMP9, and β-catenin[8,23]. Our present in vitro experiments demonstrated that midazolam treatment upregulated HIF-1α expression, potentially promoting cell migration. Midazolam administration upregulated ACE2 expression and downregulated expressions of MMP9 and β-catenin, resulting in suppressed cell proliferation.

In this study, 2-hr treatment with dexmedetomidine (0, 1, 10, 100 nM) promoted migration but not proliferation of A549 cells, upregulated ACE2 expression, and downregulated expressions of HIF-1α, MMP9, and β-catenin. In their 2018 study, Wang et al.[11] showed that 24-hr treatment with 0.001–10 nM dexmedetomidine stimulated cell proliferation and migration, which suggests that the difference in exposure time between their study and the present study could have caused cell viability changes. Another study showed that dexmedetomidine increased HIF-1α and MMP9 expressions in hypoxinized A549 cells[10]. We used 2 hr as the exposure time, under normal oxygenation, and our results indicate that dexmedetomidine can modulate pro-cancer biomarkers other than HIF-1α, MMP9, and β-catenin, leading to stimulated cell migration. However, migration pathways other than metabolic and structural signals may be involved by suppressing invasion-related markers (MMP9, β-catenin) and increasing ACE2.

The outcome of our PCR array confirmed that midazolam treatments upregulated four genes: AKT2, E2F1, FOS, and TP53. The genes AKT2, E2F1, FOS, and FZD1 promote cancer cell proliferation[24–26]. The TP53 gene is a cancer-suppressive gene that leads cancer cells to apoptosis[27]. The FZD1 gene encodes a receptor protein for the Wnt signaling protein, and FZD1 overexpression promotes cancer cell proliferation[28]. Our present data suggest that midazolam treatment promotes cell migration via increased expression of the AKT2, E2F1, and FOS genes but can also decrease cell proliferation via upregulation of the TP53 gene, indicating that activation of cell survival and proliferation-related signals may explain why migration promotion and metabolic suppression occur simultaneously. In our PCR array, dexmedetomidine upregulated the expression of the CRK and FZD1 genes. CRK acts as an adapter protein in cancer and is related to cell malignant transformation[29]. Taken together, our findings suggest that dexmedetomidine promotes migration of A549 cells by upregulating CRK and FZD1.

Study Limitations

This study had several limitations. First, it was an in vitro investigation using a single cell line. In vivo studies and studies of other cell lines are thus warranted. Second, continuous midazolam and dexmedetomidine administration, or longer durations of administration, could have altered the results and revealed the appropriate concentration and/or exposure time for cancer surgeries. Finally, our experiments did not identify a direct path-

way underlying the actions of dexmedetomidine in A549 cells.

Conclusion

Our preliminary data suggest that midazolam suppresses cell proliferation and synthesis, which would have some benefit for lung cancer surgery. Although additional studies that include other cell lines and longer follow-up, as well as in vivo studies and clinical studies, are necessary, the results of this subclinical study may aid in selecting anesthetic agents in onco-surgery.

Author Contributions: Conceptualization: M.I. (Masae Iwasaki) and M.I. (Masashi Ishikawa); Methodology: A.I, M.I. (Masashi Ishikawa), M.T., M.Y., and M.I. (Masae Iwasaki); Software: M.I. (Masae Iwasaki); Validation: A.I., M.I. (Masae Iwasaki), and M.I. (Masashi Ishikawa); Formal analysis: A.I., M.I. (Masae Iwasaki), and M.I. (Masashi Ishikawa); Investigation: A.I., M.I. (Masae Iwasaki), M.T., M.Y., and M.I. (Masashi Ishikawa); Resources: M.I. (Masae Iwasaki) and M.I. (Masashi Ishikawa); Data curation: A.I., M.I. (Masae Iwasaki), M.T., M.Y., and M.I. (Masashi Ishikawa); Writing—original draft preparation: A.I. and M.I. (Masae Iwasaki); Writing—review and editing: A.I., M.I. (Masae Iwasaki), M.Y., M.T., and M.I. (Masashi Ishikawa); Visualization: A.I., M.I. (Masae Iwasaki), and M.I. (Masashi Ishikawa); Supervision: M.I. (Masashi Ishikawa); Project administration: M.I. (Masae Iwasaki) and M.I. (Masashi Ishikawa); Funding acquisition: M.I. (Masae Iwasaki) and M.I. (Masashi Ishikawa). All authors have read and agreed to the published version of the manuscript.

Funding: This work was supported by KAKENHI grants from the Japan Society for the Promotion of Science (JSPS) (No. JP 24K12080 to M. Ishikawa and No. JP24K23394 to M. Iwasaki).

Conflict of Interest: The authors declare no conflict of interest.

Declaration of Generative AI and AI-Assisted Technologies in the Writing Process: Not Applicable.

Supplementary Material: Supplementary material associated with this article is available at https://doi.org/10.1272/jnms.JNMS.2026_93-210.

References

1. Ministry of health, Labour and Welfare (JP), Cancer and Disease Control Division. [Cancer incidence of Japan 2020] [Internet]. Tokyo: Ministry of health, Labour and Welfare, Cancer and Disease Control Division; 2020. Available from: https://www.mhlw.go.jp/content/10900000/001231386.pdf. Japanese.
2. Japan Lung Cancer Society. [Lung cancer treatment guidelines - including malignant pleural mesothelioma and thymic tumors 2022 edition] [Internet]. Tokyo: Japan Lung Cancer Society; 2022. Available from: https://www.haigan.gr.jp/guideline/2022/index.html. Japanese.
3. Iwasaki M, Edmondson M, Sakamoto A, Ma D. Anesthesia, surgical stress, and "long-term" outcomes. Acta Anaesthesiol Taiwan [Internet]. 2015 Sep;53(3):99–104. Available from: https://www.ncbi.nlm.nih.gov/pubmed/26235899
4. Ishikawa M, Iwasaki M, Sakamoto A, Ma D. Anesthetics may modulate cancer surgical outcome: a possible role of miRNAs regulation. BMC Anesthesiol [Internet]. 2021 Mar 9;21(1):71. Available from: https://www.ncbi.nlm.nih.gov/pubmed/33750303
5. Wigmore TJ, Mohammed K, Jhanji S. Long-term survival for patients undergoing volatile versus IV anesthesia for cancer surgery: a retrospective analysis. Anesthesiology [Internet]. 2016 Jan;124(1):69–79. Available from: https://www.ncbi.nlm.nih.gov/pubmed/26556730
6. Dou Y, Li Y, Chen J, et al. Inhibition of cancer cell proliferation by midazolam by targeting transient receptor potential melastatin 7. Oncol Lett [Internet]. 2013 Mar;5(3):1010–6. Available from: https://www.ncbi.nlm.nih.gov/pubmed/23426784
7. Qi Y, Yao X, Du X. Midazolam inhibits proliferation and accelerates apoptosis of hepatocellular carcinoma cells by elevating microRNA-124-3p and suppressing PIM-1. IUBMB Life [Internet]. 2020 Mar;72(3):452–64. Available from: https://www.ncbi.nlm.nih.gov/pubmed/31651086
8. Iwasaki M, Yamamoto M, Tomihari M, Ishikawa M. Ropivacaine administration suppressed A549 lung adenocarcinoma cell proliferation and migration via ACE2 upregulation and inhibition of the Wnt1 pathway. Int J Mol Sci [Internet]. 2024 Aug 28;25(17):9334. Available from: https://www.ncbi.nlm.nih.gov/pubmed/39273283
9. Talib HK, Dobesova Z, Klir P, et al. Association of red blood cell sodium leak with blood pressure in recombinant inbred strains. Hypertension [Internet]. 1992 Oct;20(4):575–82. Available from: https://www.ncbi.nlm.nih.gov/pubmed/1398893
10. Chen HY, Li GH, Tan GC, et al. Dexmedetomidine enhances hypoxia-induced cancer cell progression. Exp Ther Med [Internet]. 2019 Dec;18(6):4820–8. Available from: https://www.ncbi.nlm.nih.gov/pubmed/31772647
11. Wang C, Datoo T, Zhao H, et al. Midazolam and dexmedetomidine affect neuroglioma and lung carcinoma cell biology in vitro and in vivo. Anesthesiology [Internet]. 2018 Nov;129(5):1000–14. Available from: https://www.ncbi.nlm.nih.gov/pubmed/30157038
12. Lu HL, Wu KC, Chen CW, et al. Anticancer effects of midazolam on lung and breast cancers by inhibiting cell proliferation and epithelial-mesenchymal transition. Life (Basel) [Internet]. 2021 Dec 13;11(12):1396. Available from: https://www.ncbi.nlm.nih.gov/pubmed/34947927
13. Tam SY, Wu VWC, Law HKW. Hypoxia-induced epithelial-mesenchymal transition in cancers: HIF-1α and beyond. Front Oncol [Internet]. 2020;10:486. Available from: https://www.ncbi.nlm.nih.gov/pubmed/32322559
14. Huang H. Matrix Metalloproteinase-9 (MMP-9) as a cancer biomarker and MMP-9 biosensors: Recent advances. Sensors (Basel) [Internet]. 2018 Sep 27;18(10):3249. Available from: https://www.ncbi.nlm.nih.gov/pubmed/30262739
15. Vu TH, Shipley JM, Bergers G, et al. MMP-9/gelatinase B

is a key regulator of growth plate angiogenesis and apoptosis of hypertrophic chondrocytes. Cell [Internet]. 1998 May 1;93(3):411–22. Available from: https://www.ncbi.nlm.nih.gov/pubmed/9590175
16. Itoh T, Tanioka M, Matsuda H, et al. Experimental metastasis is suppressed in MMP-9-deficient mice. Clin Exp Metastasis [Internet]. 1999 Mar;17(2):177–81. Available from: https://www.ncbi.nlm.nih.gov/pubmed/10411111
17. Zeng ZS, Cohen AM, Guillem JG. Loss of basement membrane type IV collagen is associated with increased expression of metalloproteinases 2 and 9 (MMP-2 and MMP-9) during human colorectal tumorigenesis. Carcinogenesis [Internet]. 1999 May;20(5):749–55. Available from: https://www.ncbi.nlm.nih.gov/pubmed/10334190
18. Zhang Y, Wang X. Targeting the Wnt/β-catenin signaling pathway in cancer. J Hematol Oncol [Internet]. 2020 Dec 4;13(1):165. Available from: https://www.ncbi.nlm.nih.gov/pubmed/33276800
19. Sadot E, Geiger B, Oren M, Ben-Ze'ev A. Down-regulation of beta-catenin by activated p53. Mol Cell Biol [Internet]. 2001 Oct;21(20):6768–81. Available from: https://www.ncbi.nlm.nih.gov/pubmed/11564862
20. He S, Tang S. WNT/β-catenin signaling in the development of liver cancers. Biomed Pharmacother [Internet]. 2020 Dec;132:110851. Available from: https://www.ncbi.nlm.nih.gov/pubmed/33080466
21. Goddette DW, Frieden C. Actin polymerization. The mechanism of action of cytochalasin D. J Biol Chem [Internet]. 1986 Dec 5;261(34):15974–80. Available from: https://www.ncbi.nlm.nih.gov/pubmed/3023337
22. Zhang Q, Lu S, Li T, et al. ACE2 inhibits breast cancer angiogenesis via suppressing the VEGFa/VEGFR2/ERK pathway. J Exp Clin Cancer Res [Internet]. 2019 Apr 25;38(1):173. Available from: https://www.ncbi.nlm.nih.gov/pubmed/31023337
23. Tomihari M, Iwasaki M, Ishikawa M. Propranolol and landiolol inhibit cell proliferation enhanced by noradrenaline in human lung adenocarcinoma cells. Biomed Res [Internet]. 2024;45(6):253–9. Available from: https://www.ncbi.nlm.nih.gov/pubmed/39581614
24. Liu T, Zhu J, Du W, et al. AKT2 drives cancer progression and is negatively modulated by miR-124 in human lung adenocarcinoma. Respir Res [Internet]. 2020 Sep 1;21(1):227. Available from: https://www.ncbi.nlm.nih.gov/pubmed/32873299
25. Gobbi G, Grieco A, Torricelli F, et al. The long non-coding RNA TAZ-AS202 promotes lung cancer progression via regulation of the E2F1 transcription factor and activation of Ephrin signaling. Cell Death Dis [Internet]. 2023 Nov 18;14(11):752. Available from: https://www.ncbi.nlm.nih.gov/pubmed/37980331
26. Manios K, Tsiambas E, Stavrakis I, et al. c-Fos/c-Jun transcription factors in non-small cell lung carcinoma. J BUON [Internet]. 2020 Sep-Oct;25(5):2141–3. Available from: https://www.ncbi.nlm.nih.gov/pubmed/33277827
27. Munro AJ, Lain S, Lane DP. P53 abnormalities and outcomes in colorectal cancer: a systematic review. Br J Cancer [Internet]. 2005 Feb 14;92(3):434–44. Available from: https://www.ncbi.nlm.nih.gov/pubmed/15668707
28. Wang R, Wang X, Zhang J, Liu Y. LINC00942 promotes tumor proliferation and metastasis in lung adenocarcinoma via FZD1 upregulation. Technol Cancer Res Treat [Internet]. 2021 Jan-Dec;20:1533033820977526. Available from: https://www.ncbi.nlm.nih.gov/pubmed/34253104
29. Park T. Crk and CrkL as therapeutic targets for cancer treatment. Cells [Internet]. 2021 Mar 27;10(4):739. Available from: https://www.ncbi.nlm.nih.gov/pubmed/33801580